Impulse Response with Correlation Study of a Broadband Bended Wearable Monopole Antenna

Zahran, S. R., Abdalla, M. A. and Budimir, D.

This is a copy of the author's accepted version of a paper subsequently to be published in the proceedings of the *12th European Conference on Antennas and Propagation (EUCAP),* Excel, London, 09 to 13 Apr 2018, IEEE.

The final published version is available online at:

https://doi.org/10.1049/cp.2018.1216

Impulse Response with Correlation Study of a Broadband Bended Wearable Monopole Antenna

Sherif R. Zahran[1], Mahmoud A. Abdalla[2], and D. Budimir [3,4]

[1] Electronics and Communication Engineering Department, Arab Academy for Science, Technology and Maritime Transport, Cairo, Egypt, sherif.zahran.1991@ieee.org

[2] Electronic Engineering Department, MTC College Cairo, Egypt, maaabdalla@ieee.org

[3] Wireless Communications Research Group, University of Westminster, London, United Kingdom, d.budimir@wmin.ac.uk

[4]School of Electrical Engineering, University of Belgrade, Serbia

***Abstract*—In this paper, the impulse response of a wide band flexible circular monopole antenna is presented. The antenna is fabricated on liquid crystalline polymer flexible substrate with a compact geometry that makes it suitable for wearable applications under different bending conditions. The antenna is fed by coplanar waveguide transmission line and has a compact total size of 40 × 22 mm^2. The presented antenna has a good performance over the operating frequency range for straight and bent configurations. The design principals, simulation and experimental results are presented in this work.**

Index Terms— Monople Antennas, Impluese Response, Wearable, Flexible substrate.

I. Introduction

The need for mechanically bendable wireless devices is growing due to their wide area of applications such as wearable and implantable devices for health monitoring systems in addition to the daily life wireless devices such as cell phones, smart watches and others. For this purpose, the need for printed malleable antennas has increased recently. With the enormous bandwidth available, the capacity for high data rates and the potential for small size and low processing power, technologies that utilize wide spectrum became a widely used radio solution for future wireless indoor home-networking technology [1] and [2]. From another aspect, designing flexible antennas would require thin substrates, as a consequent the antenna's radiation pattern properties tends to be degraded [3]-[5]. Examples for flexible broadband antennas in planar configurations are pointed in [6]-[14].

Time domain investigation for broadband antennas became recently a vital study. As the radiated pulses last very short time given that huge frequency range, it is more likely to be distorted through the system. This is one reason to study UWB antennas in time domain in order to predict the produced signal as in [15]-[25].

In this work, we use a very thin substrate to demonstrate a typical wideband flexible antenna. The antenna design has been addressed and its performance has been checked using electromagnetic full wave simulations and experimental measurements. Impulse response studies in time domain for antennas in both straight and bent cases are introduced.

II. Antenna Geometry and Parameters

A. Antenna Geometry

The antenna is built upon a flexible material that satisfies robustness and can withstand thermal conditions. Rogers ultralam 3850 fulfilled the mechanical requirements at which a radiating element can perform efficiently under extreme bending. The selected material consists of 100 µm liquid crystalline polymer substrate with dielectric constant of 2.9 sandwiched by two 18 µm thick copper cladding. The antenna is existed by 50 Ω CPW transmission line with width of 2.2 mm on its edge a SMA connector was soldered using special type of liquid solder. The total size of the antenna is 40 × 22 mm^2. As shown in Fig. 1 (a), the patch antenna is designed to be typical circular monopole the labeled parameters are indicated in caption. The design of the radiating monopole dimensions is based on quarter wavelength calculations. Fig. 1 (b) and (c), represent the simulation and the measurement configuration setups while the antenna is bent respectively.

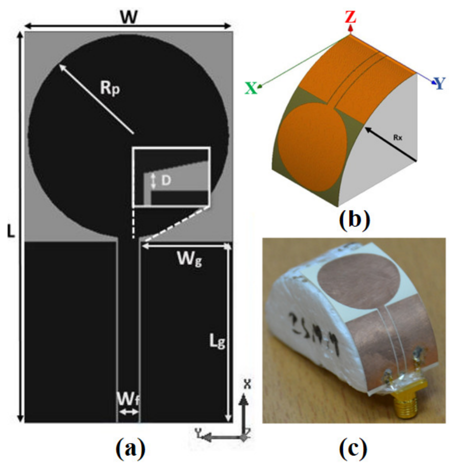

Fig. 1. The monopole antenna geometry (a) top layer latout (L = 40 mm, W = 22 mm, Lg = 18.9 mm, Wg = 9.7 mm, Rp = 10.6 mm, W_f = 2.2 mm and D = 0.45 mm), (b) the bent simulation configuration and (c) the bent fabricated antenna prototype.

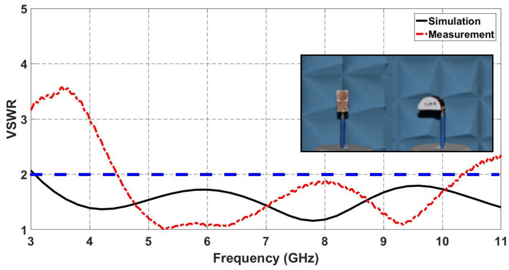

Fig. 2. Simulated and measured VSWR (subfigure: anechoic farfield measurment setup for straight and bent antenna scenarios)

It worth to mention that in practical measurement the antenna was bent upon the curved surface of a semi-cylinder with radius (Rx) 25 mm.

B. Results and Discussion

The simulated voltage standing wave ratio (VSWR) of the monopole antenna was executed using the commercial software (HFSS). Also, the measured VSWR was done using Agilent FieldFox N9918A Vector Network Analyzer. Fig. 2, represents the simulated and measured VSWR of the proposed antenna. The simulated VSWR result indicating that the associated less than value of 2 in VSWR is achieved across the entire monitored spectrum with high resonance, the antenna is well matched over the frequency range associated for the UWB spectrum (3.1 GHz – 10.6 GHz). In general, there is a good agreement between the two results in the main figure pattern. However, the measured VSWR has values greater than 3 (25 % reflected power) in the frequency range 3 GHz – 4 GHz. The discrepancies may be claimed due to the imperfection of fabrication process as a consequence of the very thin substrate of the antenna along with the available SMA connectors made it difficult to measure using the accessible measuring tools.

To investigate the radiation properties of the bent monopole antenna, two frequencies within the matching frequencies of the antenna were selected to plot its radiation pattern. These two frequencies were selected to be in the heart of the UWB spectrum. Therefore, 4 GHz and 8 GHz were selected so that the straight and bent antenna configuration radiation pattern is depicted in the subfigure of Fig. 2. The practical measurements of the pattern were done in a near field measurement system (Starlab anechoic chamber).

A comparison between measured and simulated results in the sense of total gain radiation pattern in dBi for planes X-Y and Y-Z at the investigated frequencies is introduced in Fig. 3 (a) and (b), for straight and bent antenna configuration setups respectively. Fig, 3 (a), indicates that the antenna maintains a semi omnidirectional radiation represented in figure of eight shaped pattern at X-Y plane for lower part of the spectrum and tends to deform as frequency increases. Fig. 3 (b), indicates some agreement

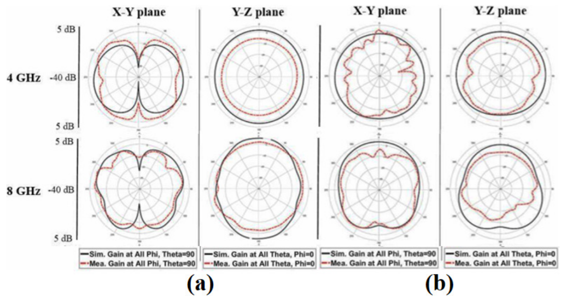

Fig. 3. Measured and simulated 2D gain radiation pattern for (a) straight antenna setup (b) bent antena setup

between gain simulation and measurement for the bent configuration in sense of gain magnitude, X-Y radiation pattern don't include any figure of eight shaped radiation pattern confirming how the produced radiation is affected by flexing the antenna.

III. IMPULSE RESPONSE CALCULATION

Utilizing the wide frequency range in which the antenna operates the signal is more likely to be distorted through the transmitting-receiving system, this is one reason to study broadband antennas in time domain in order to predict the produced signal.

The transmission coefficient S_{21} is measured between two separated identical antennas connected to VNA ports in three different configuration setups: face to face, face to side and side to side, the three S_{21} measurement setups are photographed in Fig. 4 (a), (b) and (c), respectively. Same measurement procedure was carried out one more time while the antennas were bent, Fig. 4 (d), shows the side to face configuration setup of bent antennas. The distance between the antennas is set to be 1 meter which is larger than the far field barrier radius calculated at 10 GHz (shortest wavelength in the spectrum of operation). This setup was intentionally constructed in such multi-reflections environment in order to realize the operational environment in which an indoor wearable antenna operates in.

Equation (1) represents first order Gaussian pulse with characteristic time (a=200 ps) represents the input signal is constructed. Same input signal is represented in frequency domain by applying Fast Fourier Transform in (2). Now the signal is ready to be multiplied with the system's transfer function (S_{21}) in order to extract the impulse response (IR) represented in (3). As the received signal should have lower magnitude a normalization function is utilized for both input and received signals to have a far comparison between the shapes of them as in (4). With a simple MATLAB code the system's impulse response can be calculated.

$$Input\_Signal(t) = \sin(2\pi f_0 t)\,.\,e^{-\left(\frac{t-1}{a}\right)^2} \tag{1}$$

$$Input\_Signal(\omega) = FFT(Input\_Signal(t)) \tag{2}$$

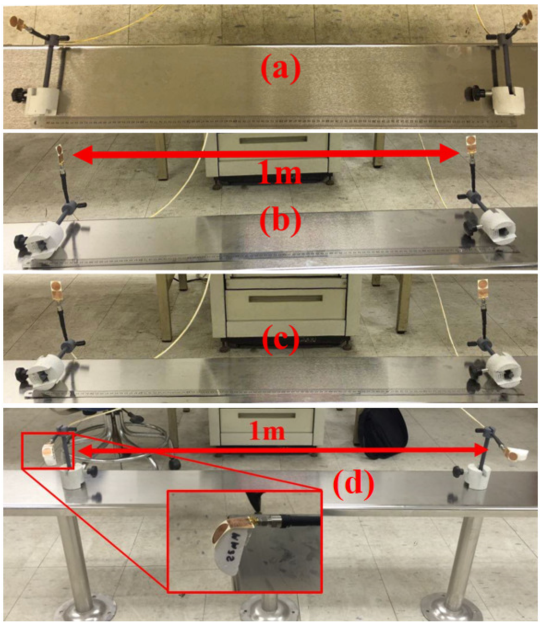

Fig. 4. Time response measurements setup for different configurations (a) face to face (straight) (b) side to face (straight) (c) side to side (straight) and (d) side to face (bent)

$$\text{Im}\,pulese\ \text{Response} = Input\_Signal(\omega).S_{21}(\omega) \tag{3}$$

$$Normalized\,\text{Im}\,pulese\ \text{Response} = \frac{\text{Im}\,pulese\ \text{Response}}{\max(\text{Im}\,pulese\ \text{Response})} \tag{4}$$

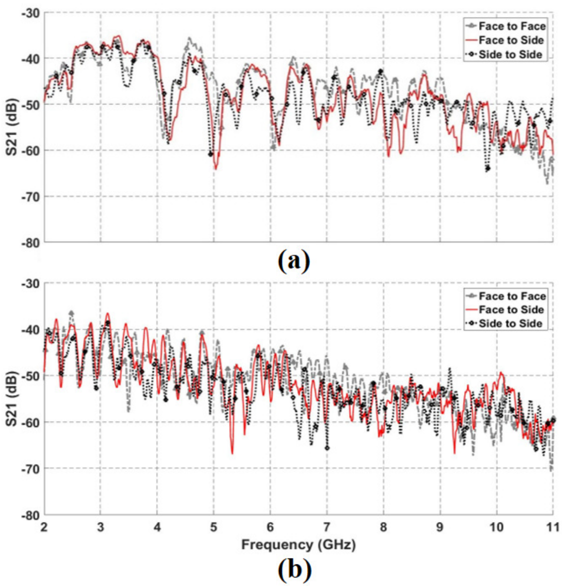

Fig. 5. Measured magnitude of S_{21} for different configuration antenna setups (a) straight (b) bent

Transfer function (S_{21}) with stable magnitude and linear in phase within operation spectrum is considered as a good impulse response indicator. It can be noticed from Fig. 5 (a) and (b), that the magnitude of S_{21} for different configurations is fluctuating between -35 and -65 dB. Fig. 6 (a) and (b), represent linearity in unwrapped phase for both straight and bent scenarios. As observed in Fig. 6 (a), that face to face and face to side scenarios coincide in phase while side to side setup's phase shows minor increase in its slope after 6 GHz. This is due to some deformation in the radiation pattern at higher frequencies compared to lower one as depicted in Fig. 3 (a). This problem becomes more crucial if the magnitude of radiation is small in the case of direct transmission as the case of side to side. Fig. 6 (b), represents considerable linearity of unwrapped phase in radians for face to face and side to side scenarios in which they almost coincide in phase while face to side setup's phase shows higher slope. This deviation is considered due to the deformation of face to side radiation pattern generated from bent antenna as shown in Fig. 3 (b).

To conclude, a comparison between acquired data is conducted in order to check the functionality of the studied wideband antenna, Fig. 7 (a) and (b), represents the input signal along with the calculated (simulated and measured) received pulses for the three setups of straight and bent antennas respectively, noting that the received pulses are delayed by 3 ns in order to illustrate any distortions, it is observed that received signals are highly correlated to the input signal except for minor distorted repels and side ringing patterns.

Finally Table I and II, represents the values of the cross correlation between input signal and received pulses

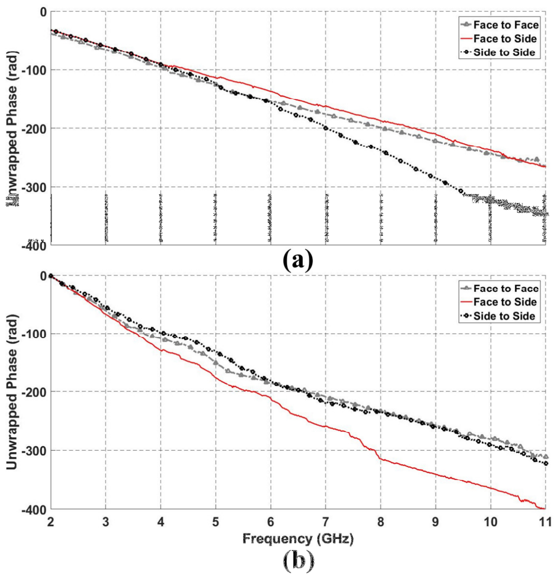

Fig. 6. Measured phase of S_{21} (unwrapped) for different configuration antenna setups (a) straight (b) bent

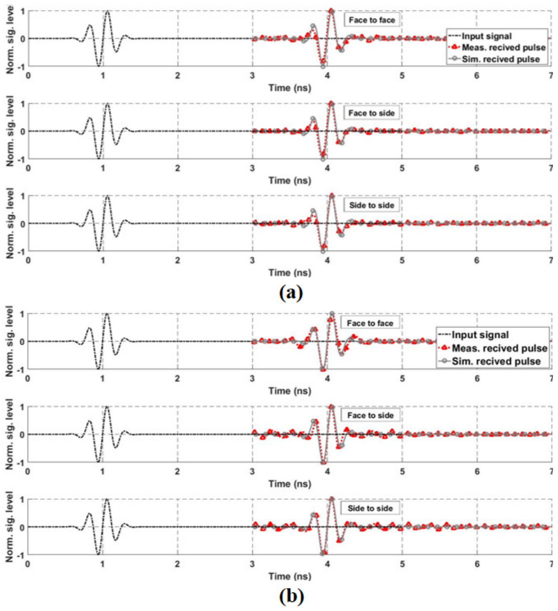

Fig. 1. Simulation and measurement of the normlized received pulse for different configuration setups (straighht antenna)

(simulated and measured) for straight and bent antennas scenarios respectively.

TABLE I. PULSE CROSS CORRELATION FOR STRAIGHT ANTENNA CONFIGURATRION

	Received pulses and input signal correlation		
	Face to face	***Face to side***	***Side to side***
Simulation	0.9977	0.9994	0.9979
Measurement	0.9210	0.9195	0.9640

TABLE II. PULSE CROSS CORRELATION FOR BENT ANTENNA CONFIGURATION

	Received pulses and input signal correlation		
	Face to face	***Face to side***	***Side to side***
Simulation	0.9994	0.9887	0.9992
Measurment	0.9256	0.9298	0.9441

IV. CONCLUSION

A typical circular monopole CPW-fed antenna fabricated using flexible LCP substrate has been presented in this paper. The simulation and measurement for both straight planar and bent scenarios have been conducted. The VSWR results indicate that the antenna is well matched over the frequency range associated for the UWB technology. Anechoic chamber measurement of the far field characteristics showed semi omni-directive radiation pattern at lower frequencies. Impulse response studies in time domain were conducted, the received simulated and measured pulses from different setup scenarios showed high cross correlation with the input pulse with variant small degradation in proportional with antenna setup. The antenna even under bending conditions considering its compact size and basic design is suitable for commercial wearable applications.

REFERENCES

[1] P.S. Hall, Y. Hao, “Antennas and Propagation for Body-Centric Wireless Communications, Second Edition” Artech House, 2011.

[2] D.H. Werner, Z.H. Jiang, “Electromagnetics of Body Area Networks: Antennas, Propagation, and RF Systems”, John Wiley & Sons, 2016.

[3] H.R. Raad, A.I. Abbosh, H.M. Al-Rizzo, D.G. Rucker, "Flexible and Compact AMC Based Antenna for Telemedicine Applications", IEEE Trans. Ant. Propag., vol. 61, no. 2, pp. 524 - 531, 2013.

[4] Y.H. Jung, Y. Qiu, S. Lee, T.Y. Shih, Y. Xu, "A Compact Parylene-Coated WLAN Flexible Antenna for Implantable Electronics", IEEE Ant. Wireless Propag. Lett., vol. 15, pp. 1382 - 1385, 2016.

[5] S. Hong, S.H. Kang, Y. Kim, C. W. Jung, "Transparent and Flexible Antenna for Wearable Glasses Applications", IEEE Trans. Ant. Propag. , vol. 64, no. 7, pp. 2797 - 2804, 2016.

[6] A.A. Gheethan and D.E. Anagnostou, "Dual Band-Reject UWB Antenna with Sharp Rejection of Narrow and Closely-Spaced Bands" IEEE Trans. Ant. and Prop. , vol. 60, no. 4, pp. 2071 - 2076, 2012.

[7] C.P. Deng, X.Y. Liu, Z.K. Zhang, M.M. Tentzeris, "A Miniascape-Like Triple-Band Monopole Antenna for WBAN Applications", IEEE Ant. Wireless Propag. Lett., vol. 11, pp. 1330 – 1333, 2012.

[8] P.B. Samal, P.J. Soh, G.A. Vandenbosch, "UWB All-Textile Antenna With Full Ground Plane for Off-Body WBAN Communications", IEEE Trans. Ant. Propag. , vol. 62, no. 1, pp. 102 - 108, 2014

[9] Q.H. Abbasi, M. UrRehman, X. Yang, A. Alomainy, K. Qaraqe, E. Serpedin, "Ultrawideband Band-Notched Flexible Antenna for Wearable Applications", IEEE Ant. and Wireless Prop. Lett., vol. 12, pp. 1606 - 1609, 2013

[10] H.R. Khaleel, "Design and Fabrication of Compact Inkjet Printed Antennas for Integration within Flexible and Wearable Electronics", IEEE Trans Comp. Pack. Manufa. Tech., vol. 4, no. 10, pp. 1722 - 1728, 2014

[11] Y. Qiu, Y.H.Jung, S. Lee, T.Y. Shih, J. Lee, Y.H.Xu, R. Xu, W. Lin, N. Behdad, Z. Ma, "Compact parylene-c-coated flexible antenna for WLAN and upper-band UWB applications", Elec. Lett., vol. 50 no. 24, pp. 1782–1784, 2014.

[12] Y. Sun, S.W. Cheung, T.I. Yuk, "Design of a textile ultra-wideband antenna with stable performance for body-centric wireless communications", IET Microw. Ant. Propag., vol. 8, no. 15, pp. 1363–1375, 2014.

[13] S. Nikolaou, G.E. Ponchak, J. Papapolymerou and M.M. Tentzeris, "Conformal Double Exponentially Tapered Slot Antenna (DETSA) on LCP for UWB Applications", IEEE Trans. Ant. and Propag. , vol. 54, no. 6, pp. 1663 - 1669, 2006.

[14] M. El Atrash, K. Bassem, M.A. Abdalla, "A Compact Dual-Band Flexible Cpw-Fed Antenna For Wearable Applications", 2017 IEEE AP-S Int. Ant. Propag. Symp. Digest, July 2017, San Deigo, USA, pp. 2463–2464.

[15] C.J Lei, Z.W. Xia, Z. Zheng, "A Compact Band-Rejected UWB Antenna Design With Time Domain Analysis", IEEE Int. Symp.on KAM Workshop, pp. 243-270, 2008.

[16] G. Quintero, J.F. Zürcher, A.K. Skrivervik, "System Fidelity Factor: A New Method For Comparing UWB Antennas", IEEE Trans. Ant. Propag., vol. 59, no. 7, pp. 2502-2512, July 2011

[17] H.K. Yoon, Y.J. Yoon, H. Kim and C.-H. Lee, "Flexible Ultra-Wideband Polarisation Diversity Antenna With Band-Notch Function", IET Microw. Ant. Propag., vol. 5, no. 12, pp. 1463-1470, March 2011.

[18] G. Clementi, N. Fortino, J.Y. Dauvignac, and G. Kossiavas, "Frequency and Time Domain Analysis Of Different Approaches To The Backing Of An UWB Slot Antenna", IEEE Trans. Ant. Propag., vol. 60, no. 7, pp. 3495-3498. July 2012.

[19] G.P. Gao, B.Hu, J.S. Zhang, "Design of a Miniaturization Printed Circular-Slot UWB Antenna By The Half-Cutting Method", IEEE Ant. Wireless Propag.Lett., vol. 12, pp. 567-570, 2013.

[20] G.K. Pandey, H.S. Singh, P.K. Bharti and M.K. Meshram, "Metamaterial-Based UWB Antenna", Elect. Lett., vol. 50, no. 18 pp. 1266–1268, August 2014.

[21] M.Ur-Rehman, Q.H. Abbasi, M. Akram and C.Parini, "Design Of Band-Notched Ultra Wideband Antenna For Indoor And Wearable Wireless Communications", IET Microw., Ant. Propag., August 2014

[22] A.M. Abdelraheem and M.A. Abdalla, "Compact Curved Half Circular Disc-Monopole UWB Antenna", Int. J. of Microw. and Wireless Tech., vol. 8, no. 2, pp. 283-290, 2016.

[23] M. N. Srifi, S.K. Podilchak, M. Essaaidi and Y.M. Antar, "Compact Disc Monopole Antennas for Current and Future Ultrawideband (UWB) Applications", IEEE Trans. Ant. Propag., vol. 59, no. 12, PP. 4470 – 4480, December 2011.

[24] Q. Bonds, T. Weller and H. Arslan, "An Ultra-Wideband (UWB) Pulse Dispersion Study For Antennas In Sensor Network Applications", IEEE Ant. Propag. Society Int. Symp., 2007, pp. 1429-1432.

[25] A. Adelraheem, M. Abdalla, H.Elregaily, A. Mitkees, "Experimental Evaluation Of High-Fidelity High-Data-Rate UWB Antenna System", 2015 IEEE AP-S Int. Ant.Propag.Symp. Digest, July 2015, Vancouver, Canada, pp. 522- 523.